Supplementary Information

Experimental Section

1. Synthesis of CeO_2 octahedrons

$Ce(NO_3)_3 \cdot 6H_2O$ (1.30 g) was dissolved in 30 mL of deionized water followed by the addition of Na_3PO_4 solutions (10 mL, 5 mM) and stirred for 30 min. Then, the mixture solution was sealed in a 50 mL teflon-lined stainless autoclave and heated at 170 °C for 24 h.

2. Synthesis of CeO_2 nanowires

$Ce(NO_3)_3 \cdot 6H_2O$ (0.43 mg) was dissolved in 5 mL of deionized water followed by the addition of NaOH solutions (35 mL, 6.5 M) and stirred for 30 min. Then, the mixture solution was sealed in a 50 mL teflon-lined stainless autoclave and heated at 100 °C for 48 h.

3. Synthesis of CeO_2@MnO_2 nanostructures

As-prepared CeO_2 nanostructures (25 mg) were dispersed in $KMnO_4$ solutions (35 mL, 0.01 M). Then, the mixture solution was sealed in a 50 mL teflon-lined stainless autoclave and heated at 140 °C for 12 h.

4. Materials Characterization

The crystallographic information and chemical composition of as-prepared products were established by powder X-ray diffraction (XRD, D/max 2500, Cu Ka). The morphological and structural investigations of the CeO_2@MnO_2 nanostructures were examined by high-resolution transmission electron microscopy (HRTEM, ZEISS LIBRA 200).

5. Electrochemical measurement

A three-electrode configuration was used to measure the electrochemical properties of the structures in Na_2SO_4 (1 M) solution, where a mixture of CeO_2@MnO_2 nanostructures, acetylene black and polyvinylidene difluoride (PVDF) (7:2:1 wt%), a platinum plate and a saturated calomel electrode (SCE) were used as working, counter and reference electrodes, respectively. The electrolytic cell was obtained from Cells Electrochemistry Experiment Equipments Co., Ltd., China (www.hzcell.com). The asymmetric supercapacitor was measured with a two-electrode system, including CeO_2 nanowire@MnO_2 nanostructures as the positive electrode, a Whatman filter paper as separator, and AGO as the negative electrode.

The electrochemical performances in both three-electrode and two-electrode configurations were carried out on a CHI 660E electrochemical station. Cycle voltammetry (CV) and Galvanostatic charge–discharge experiments were enforced to reflect the electrochemical properties of the electrodes. EIS measurements were carried out by applying an AC voltage with 5 mV amplitude in a frequency range from 0.01 Hz to 100 kHz at the open potential.The discharge specific capacitance was calculated according to the following equation (1)

$$Csp = I\Delta t/(m\Delta V) \qquad (1)$$

where I (A) is the charge–discharge current, ΔV (V) is the tested potential range, Δt (s) is the discharge time, and m (g) is the mass of single electrode. The energy density value was calculated according to Equation (2)

$$E=0.5\ CV^2/3.6 \qquad (2)$$

where C is the capacitance (F g^{-1}) of the supcapacitor and V is its operating potential window,

respectively. The average power density value was calculated according to Equation (2) and (3):

$$P=3600\ E/t \qquad (3)$$

where t is the discharge time (s).

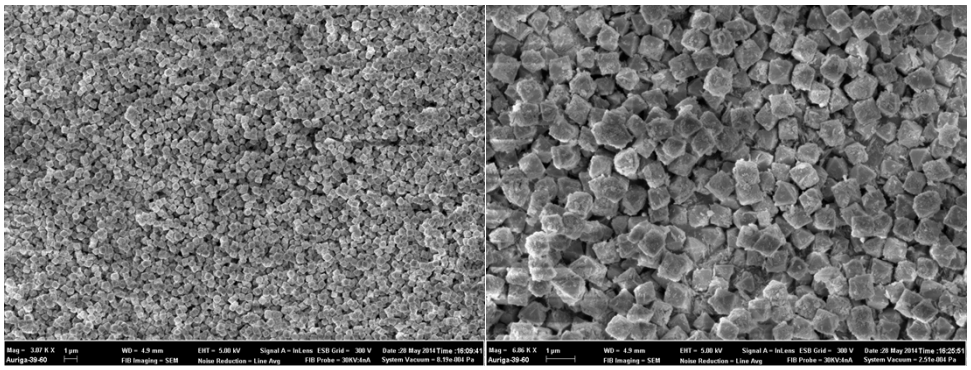

Fig .S1 SEM images of CeO_2 octahedrons

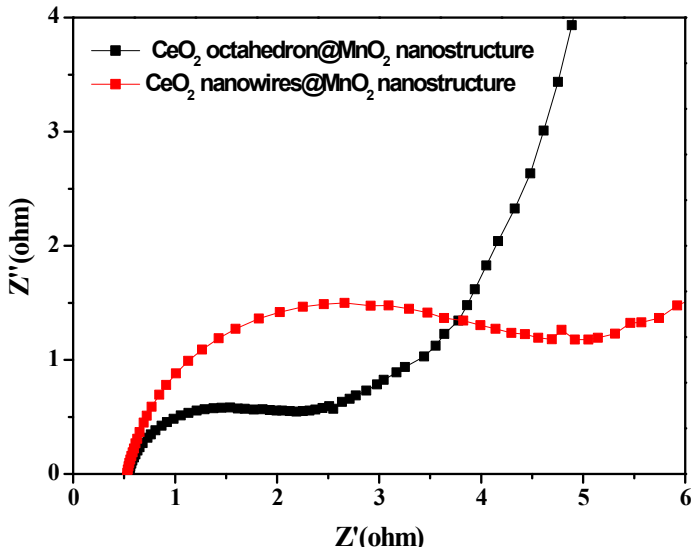

Fig .S2 Nyquist plots of the two kinds of nanostructures.

Table S1. Comparison of specific capacitances of the reported MnO_2 electrodes and the present work. All values are measured using the three-electrode system.

samples	C（Fg-1）	Electrolyte	Testing condition	references
Amorphous MnO_2	110	2 M NaCl	5 mV s^{-1}	1
Birnessite MnO_2	110	0.1 M K_2SO_4	2 mV s^{-1}	2
α-MnO_2 hollow urchins	123	0.5 M Na_2SO_4	2 mV s^{-1}	3
Ambigel MnO_2	130	2 M NaCl	5 mV s^{-1}	4
α-MnO_2 nanorod	152	1 M Na_2SO_4	5 mV s^{-1}	5
MnO_2 nanorod	168	1 M Na_2SO_4	5 mV s^{-1}	6
MnO_2 nanowire	176	1 M Na_2SO_4	5 mV s^{-1}	7
MnO_2 nanosheet	182	0.1 M Na_2SO_4	0.1 A g^{-1}	8
GHCS/MnO_2	184	1 M Na_2SO_4	0.1 A g^{-1}	9
MnO_2 microsphere	190	1 M Na_2SO_4	0.5 A g^{-1}	10
MnO_2/CNTs/RGO	193	1 M Na_2SO_4	0.2 A g^{-1}	11
α-MnO_2 sphere	200	0.25 M Na_2SO_4	1 A g^{-1}	12
Graphene/Honeycomb MnO_2	210	1 M Na_2SO_4	0.5 A g^{-1}	13
α-MnO_2 nanorod	245	1 M KOH	1 A g^{-1}	14
α- MnO_2 spherical-like particle	258.7	1 M Na_2SO_4	0.1 A g^{-1}	15
Graphene Hydrogel/ MnO_2	266.8	0.5 M Na_2SO_4	1 A g^{-1}	16
Mesoporous α-MnO_2 network	283	1 M Na_2SO_4	2 mV s^{-1}	17
MnO_2 nanowire	300	1 M Na_2SO_4	5 mV s^{-1}	18
MnO_2 tubular nanostructure	315	1 M Na_2SO_4	0.2 A g-1	19
α-MnO_2 ultralong nanowire	345	0.5 M Na_2SO_4	1 A g^{-1}	20
MnO_2 nanoflower	347	1 M Na_2SO_4	5 mV s^{-1}	21
MnO_2 hollow structure	366	1 M Na_2SO_4	5 mV s^{-1}	22
Co_3O_4/MnO_2	480	1 M LiOH	2.67 A g^{-1}	23
CeO_2 octahedron@MnO_2 nanostructure	178.5	1 M Na_2SO_4	0.25 A g^{-1}	
CeO_2 nanowire@MnO_2 nanostructure	255.2	1 M Na_2SO_4	0.25 A g^{-1}	

By comparison, we find the CeO_2@MnO_2 nanostructure are disadvantaged based on the whole weight of the samples. However, the capacitance of CeO_2 octahedron@MnO_2 nanostructures and CeO_2 nanowire@MnO_2 nanostructures calculated are 826.4 F $g^{-1}$and 622.4 F g^{-1} based on the weight of MnO_2 which is approach to the theoretical capacity of MnO_2. (The weight content of MnO_2 is calculated to be 21.6% and 41% for CeO_2 octahedron@MnO_2 nanostructures and CeO_2 nanowire@MnO_2 nanostructures respectively by treating these nanostrucures in 1 M HCl solution.)

References

1. R. N. Reddy and R. G. Reddy, *J. Power Sources*, 2004, **132**, 315-320.
2. T. Brousse, M. Toupin, R. Dugas, L. Athouël, O. Crosnier and D. Bélanger, *J. Electrochem. Soc.*, 2006, **153**, A2171-A2180.
3. J.-G. Wang, Y. Yang, Z.-H. Huang and F. Kang, *Mater. Chem. Phys.*, 2013, **140**, 643-650.
4. R. N. Reddy and R. G. Reddy, *J. Power Sources*, 2003, **124**, 330-337.
5. N. Tang, X. Tian, C. Yang and Z. Pi, *Materials Research Bulletin*, 2009, **44**, 2062-2067.
6. V. Subramanian, H. Zhu, R. Vajtai, P. Ajayan and B. Wei, *The Journal of Physical Chemistry B*, 2005, **109**, 20207-20214.
7. R. Jiang, T. Huang, J. Liu, J. Zhuang and A. Yu, *Electrochim. Acta*, 2009, **54**, 3047-3052.
8. H. Jang, S. Suzuki and M. Miyayama, *J. Electrochem. Soc.*, 2012, **159**, A1425-A1430.
9. Z. Lei, J. Zhang and X. S. Zhao, *J. Mater. Chem.*, 2012, **22**, 153.
10. W.-Y. Ko, L.-J. Chen, Y.-H. Chen, W.-H. Chen, K.-M. Lu, J.-R. Yang, Y.-C. Yen and K.-J. Lin, *J. Phys. Chem. C*, 2013, **117**, 16290-16296.
11. Z. Lei, F. Shi and L. Lu, *ACS Appl Mater Interfaces*, 2012, **4**, 1058-1064.
12. Y. Zhang, C. Sun, P. Lu, K. Li, S. Song and D. Xue, *CrystEngComm*, 2012, **14**, 5892-5897.
13. J. Zhu and J. He, *ACS Appl Mater Interfaces*, 2012, **4**, 1770-1776.
14. Z. Song, W. Liu, M. Zhao, Y. Zhang, G. Liu, C. Yu and J. Qiu, *J. Alloys Compd.*, 2013, **560**, 151-155.
15. Y. Zhang, G.-y. Li, Y. Lv, L.-z. Wang, A.-q. Zhang, Y.-h. Song and B.-l. Huang, *Int. J. Hydrogen Energy*, 2011, **36**, 11760-11766.
16. H. Gao, F. Xiao, C. B. Ching and H. Duan, *ACS Appl Mater Interfaces*, 2012, **4**, 2801-2810.
17. L. L. Yu, J. J. Zhu and J. T. Zhao, *European Journal of Inorganic Chemistry*, 2013, **2013**, 3719-3725.
18. H.-S. Nam, J.-K. Yoon, J. M. Ko and J.-D. Kim, *Mater. Chem. Phys.*, 2010, **123**, 331-336.
19. J. Zhu, W. Shi, N. Xiao, X. Rui, H. Tan, X. Lu, H. H. Hng, J. Ma and Q. Yan, *ACS App.l Mater. Interfaces*, 2012, **4**, 2769-2774.
20. W. Li, Q. Liu, Y. Sun, J. Sun, R. Zou, G. Li, X. Hu, G. Song, G. Ma and J. Yang, *J. Mater. Chem.*, 2012, **22**, 14864-14867.
21. G. Zhu, L. Deng, J. Wang, L. Kang and Z.-H. Liu, *Colloids and Surfaces A: Physicochemical and Engineering Aspects*, 2013, **434**, 42-48.
22. Y. Gu, J. Cai, M. He, L. Kang, Z. Lei and Z.-H. Liu, *J. Power Sources*, 2013, **239**, 347-355.
23. J. Liu, J. Jiang, C. Cheng, H. Li, J. Zhang, H. Gong and H. J. Fan, *Adv Mater*, 2011, **23**, 2076-2081.